How Flexibility Can Enhance Catalysis

Olivier Rivoire
Center for Interdisciplinary Research in Biology (CIRB), Collège de France, CNRS, INSERM, and Gulliver, CNRS, ESPCI, Université Paris Sciences et Lettres, 75005 Paris, France

(Received 16 December 2022; accepted 28 July 2023; published 23 August 2023)

Conformational changes are observed in many enzymes, but their role in catalysis is highly controversial. Here we present a theoretical model that illustrates how rigid catalysts can be fundamentally limited and how a conformational change induced by substrate binding can overcome this limitation, ultimately enabling barrier-free catalysis. The model is deliberately minimal, but the principle it illustrates is general and consistent with unique features of proteins as well as with previous informal proposals to explain the superiority of enzymes over other classes of catalysts. Implementing the discriminative switch suggested by the model could help overcome limitations currently encountered in the design of artificial catalysts.

DOI: 10.1103/PhysRevLett.131.088401

Enzymes can accelerate chemical reactions to a level currently unmatched by artificial catalysts from heterogeneous catalysis [1], supramolecular chemistry [2], catalytic antibodies [3], or computational protein design [4]. Could it be that enzymes follow different principles [5–7], or are they simply better [8]? An often-cited difference between enzymes and other catalysts is that enzymes commonly exhibit conformational changes, including along their catalytic cycle [9], while artificial catalysts are generally rigid. Following the principle of transition state stabilization—the cornerstone of catalysis theory—indeed leads to the design of rigid catalysts [3,4,10]. On the other hand, the role that flexibility, i.e., degrees of freedom internal to the catalyst, may play in enzyme catalysis is currently very controversial [11–13].

To date, the problem has been studied primarily by experimental and computational studies of model enzymes, with general arguments remaining informal [5–8,13,14]. Efforts to develop theoretical physics models mostly date from the 1970s and have left the issue unsettled [15]. Inspired by the power of simple physical models to clarify the mechanisms of protein folding [16] and allostery [17], we use here a minimal model of catalysis to demonstrate in the simplest and clearest terms how catalysis can benefit from a particular form of flexibility where a switch occurs between conformations of very different energy.

This approach extends our previous studies of complete catalytic cycles with simple physical models that take into account both geometric and energy constraints [18,19]. These works showed that flexibility is not necessary for catalysis and could even be detrimental: the best catalysts that were found were rigid, with no internal degree of freedom. As solid surfaces in heterogeneous catalysis, they verify the Sabatier principle [20,21]: they cannot lower the energy barrier of a reaction without limiting the desorption of products. Enzymes, on the other hand, are not subject to this trade-off and can reach a diffusion limit where the only limitation is the rate of encounter with the reactants [22]. We show here how this is possible with a particular form of flexibility that we call a discriminative switch.

To explore the design space of catalysts beyond rigid constructs, a general but tractable modeling framework is needed. Our previous models were either limited to one dimension [18] or required molecular dynamics simulations [19]. Here we reformulate the problem with a lattice model amenable to efficient and accurate calculations. This model recapitulates our previous results and extends them in two aspects. First, it allows us to identify a limit on the efficiency of rigid catalysts. To this end, we quantify the extent a to which catalysis reduces the activation energy of a reaction (the energy that appears in Arrhenius law) from a value h_s^+ in the absence of catalyst to a lesser value ah_s^+ with $a < 1$ in its presence. We show that a has a nonzero lower bound when the catalyst is rigid. Second, our model allows us to expose a generic principle by which a conformational switch can overcome this limit and enable barrier-free catalysis, with $a = 0$. This principle formalizes a key difference between biological and nonbiological catalysts.

Spontaneous reaction.—As in our previous works [18,19], we consider as a spontaneous reaction the dissociation of a dimer into its two constituent monomers but here on a lattice with two particles interacting through a potential $E_s(d_s)$ that is a function of their distance d_s in the lattice [Fig. 1(a)]. The potential excludes two particles from the same site and has two minima, at $d_s = 1$ for the dimer and at $d_s \geq 3$ for the free monomers, with an intermediate transition state at $d_s = 2$. We parametrize this potential by the forward and backward potential barriers h_s^+ and h_s^-.

The position of particle i is denoted x_i ($i = 1, 2$). The joint positions $x = (x_1, x_2)$ of the two particles on the lattice define a configuration with associated energy $E(x) = E_s(d_s)$. Each particle can independently hop to a neighboring lattice site to lead to a new configuration y.

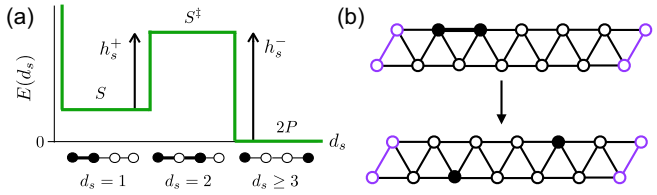

FIG. 1. Model for the spontaneous reaction. (a) Potential of interaction between two particles as a function of their distance d_s, parametrized by the barriers $h_s^\pm$. No two particles can occupy the same site and therefore $E_s(d_s = 0) = \infty$. (b) Two particles occupy distinct sites on a triangular lattice with 12 nodes and periodic boundary conditions along one direction (repeated purple nodes). The particles initially form a dimer ($d_s = 1$, with energy $h_s^- - h_s^+$; e.g., top configuration). Each particle can diffuse to a neighboring site with rates given by Metropolis rule. The reaction is completed when the particles are free ($d_s \geq 3$, energy 0; e.g., bottom configuration). This requires crossing a transition state ($d_s = 2$, energy h_s^-) and takes a mean time $T_{S\to 2P}$ that scales as $T_{S\to 2P} \sim e^{h_s^+}$ for large h_s^+.

This is taken to occur with a Metropolis rate, $k(x \to y) = k_0 \min(1, e^{-[E(y)-E(x)]/k_B T})$, where k_0 sets the unit of time and T the temperature, which we fix to $k_0 = 1$ and $k_B T = 1$. Other dynamics could be chosen, e.g., Glauber dynamics, the essential feature being that the dynamics is governed by a master equation satisfying the detailed balance, of the form $\partial_t \pi = Q^\top \pi$, where $\pi(x, t)$ is the probability to be in configuration x at time t and where $Q_{xy} = k(x \to y)$ for $x \neq y$ with $\sum_y Q_{xy} = 0$. Starting from any configuration x where the particles are bound ($d_s = 1$), we consider the first time at which the particles are free ($d_s = 3$). These sets of initial and final configurations are denoted S and $2P$. Averaging the times over all initial configurations S and over all trajectories ending in $2P$ defines the mean first-passage time $T_{S\to 2P}$, which quantifies the rate of the spontaneous reaction [19,23].

One approach to estimate $T_{S\to 2P}$ is to perform kinetic Monte Carlo simulations [24]. For our purposes, as the geometry of the lattice is not critical, we consider a small triangular lattice with $N = 12$ sites [Fig. 1(b)] for which we compute $T_{S\to 2P}$ directly by solving the set of linear equations $\sum_{y\notin 2P} Q_{xy} T_{y\to 2P} = -1$ [25,26], from which $T_{S\to 2P}$ is obtained by averaging $T_{x\to 2P}$ over all x in S [see Supplemental Material (SM) [27]].

An analytical solution can also be obtained in the limit of high reaction barriers ($h_s^+ \gg 1$) when diffusion is negligible compared to barrier crossing and all configurations of same energy are effectively equivalent [28,29]. The dynamics then reduces to a three-state Markov chain,

$$S \underset{\rho_{-1}}{\overset{\rho_1}{\rightleftharpoons}} S^\ddagger \underset{\rho_{-2}}{\overset{\rho_2}{\rightleftharpoons}} 2P, \tag{1}$$

where S represents bound configurations ($d_s = 1$), $S^\ddagger$ those in the transition state ($d_s = 2$), and $2P$ those where the particles are free ($d_s \geq 3$). Assuming instantaneous diffusion at rate 1, the transition rates between these states are simply $\rho_1 = e^{-h_s^+}$, $\rho_{-1} = \rho_2 = 1$, and $\rho_{-2} = e^{-h_s^-}$. $T_{S\to 2P}$ is then the solution of just two linear equations which can be solved analytically to yield $T_{S\to 2P} = 1/\rho_1 + 1/\rho_2 + \rho_{-1}/(\rho_1\rho_2)$ (see SM [27]). Given the assumption $h_s^+ \gg 1$, we verify Arrhenius law $T_{S\to 2P} \simeq 1/\rho_1 = e^{h_s^+}$ with h_s^+ defining the activation energy for the reaction in the absence of catalyst.

Rigid catalysis.—A catalyst effectively reduces this activation energy without being modified in the process. Inspired by heterogeneous catalysis where catalysts are solid surfaces, we first consider a catalyst consisting of two binding sites at fixed locations on the lattice [Fig. 2(a)]. When a particle occupies a binding site, the energy is lowered by ϵ_{cs}, which represents the substrate-catalyst interaction energy [Fig. 2(b)]. The distance between the binding sites is fixed to $L_c = 2$, which is the only value of L_c at which catalysis can occur: if $L_c = 1$, binding to both sites stabilizes the dimer and therefore increases the activation energy, while if $L_c \geq 3$, the binding sites cannot

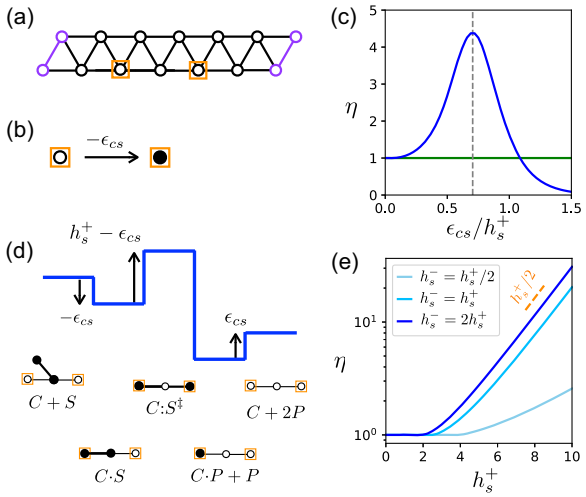

FIG. 2. Model for rigid catalysis. (a) A catalyst consists in two binding sites at fixed locations on the lattice (orange squares). (b) When a particle occupies one of these sites, the energy is decreased by ϵ_{cs}. (c) Catalytic efficiency $\eta = T_{S\to 2P}/T_{C+S\to C+2P}$ comparing the mean reaction time in this model, $T_{C+S\to C+2P}$, with the mean time $T_{S\to 2P}$ for the spontaneous reaction (Fig. 1) as a function of the binding strength ϵ_{cs} ($h_s^+ = 6$ and $h_s^- = 12$). This graph is comparable to so-called volcano plots in heterogeneous catalysis [30]. (d) Energy landscape illustrating how a rigid catalyst replaces the single barrier h_s^+ [Fig. 1(a)] by two smaller barriers $h_s^+ - \epsilon_{cs}$ and ϵ_{cs}. The occupation of the binding sites in each configuration is represented at the bottom. (e) Catalytic efficiency of optimal rigid catalysts as a function of the forward barrier h_s^+ for different reverse barrier h_s^-, showing that catalysis involves a threshold beyond which the efficiency scales exponentially.

impact the transition from $d_s = 1$ to $d_s = 2$. A geometry with $L_c = 2$ is consistent with Pauling principle [10] which states that a catalyst should be complementary to the transition state, here $d_s = 2$.

By definition, catalysis occurs when the reaction is completed faster in the presence of the binding sites than in their absence. The rate of the catalyzed reaction is estimated by a mean first-passage time denoted $T_{C+S\to C+2P}$, which is defined and obtained as $T_{S\to 2P}$, except that we account for the interaction with the binding sites when computing the energy $E(x)$ of a configuration x, and that we restrict the initial and final configurations $C + S$ and $C + 2P$ to configurations with no particle at any of the binding sites. We find that catalytic efficiency, defined by $\eta = T_{S\to 2P}/T_{C+S\to C+2P}$, can be >1 (the definition of catalysis) with an optimum at an intermediate value of ϵ_{cs} [Fig. 2(c)].

This result captures Sabatier principle [20]: an efficient catalysis must neither bind too weakly nor too strongly to the substrate. This principle is widely observed in heterogeneous catalysis [21] and was also observed in previous off-lattice models where the optimal catalysts similarly consisted of two rigidly held binding sites [18,19]. Furthermore, we observe that catalysis ($\eta > 1$) depends not only on the forward reaction barrier h_s^+, but also on the reverse barrier h_s^-, and that $\eta \leq e^{h_s^+/2}$ [Fig. 2(e)], indicating that the activation energy is at best reduced by a factor $a = 1/2$.

These observations are rationalized by studying analytically the limit of high reaction barriers ($h_s^+ \gg 1$). In this limit, the dynamics can again be reduced to a Markov process with only few states, this time five,

$$C + S \underset{\rho_{-1}}{\overset{\rho_1}{\rightleftharpoons}} C{\cdot}S \underset{\rho_{-2}}{\overset{\rho_2}{\rightleftharpoons}} C{:}S^{\ddagger} \underset{\rho_{-3}}{\overset{\rho_3}{\rightleftharpoons}} C{\cdot}P + P \underset{\rho_{-4}}{\overset{\rho_4}{\rightleftharpoons}} C + 2P, \qquad (2)$$

where $C + S$ represents configurations with a dimer ($d_s = 1$) occupying none of the binding sites, $C{\cdot}S$ those with a dimer occupying one binding site, $C{:}S^{\ddagger}$ those where the two binding sites are occupied (and therefore $d_s = 2$), $C{\cdot}P + P$ those where the particles are unbound ($d_s \geq 3$) but one occupies a binding site, and $C + 2P$ those where the particles are unbound and none occupies a binding site.

Given the correspondence between energies and rates, the states and rates can be represented by an energy landscape [Fig. 2(d)]. This representation illustrates how catalysis by two rigidly held binding sites works: it replaces the single energy barrier h_s^+ of the spontaneous reaction [Fig. 1(a)] by two smaller energy barriers [Fig. 2(c)], a barrier $h_s^+ - \epsilon_{cs}$ from $C{\cdot}S$ to $C{:}S^{\ddagger}$ and a barrier ϵ_{cs} from $C{\cdot}P + P$ to $C + 2P$. Increasing ϵ_{cs} decreases the first barrier but increases the second, which is the trade-off known as Sabatier principle [20] and the reason for the nontrivial optimum in Fig. 2(b).

In the limit $h_s^+ \gg 1$, the dynamics is controlled by the highest barrier and the optimum is therefore when the two barriers are the same, which gives $\epsilon_{cs} = h_s^+/2$. This explains why the activation energy can be lowered by a factor $a = 1/2$ at best. This result is consistent with the one obtained in an off-lattice model, where $a \simeq 0.56$ at best [19]. For this optimum to be reached, the backreaction $C{\cdot}P + P \to C{:}S^{\ddagger}$ must be negligible, or time is spent recrossing the barriers. This explains the role played by the reverse barrier h_s^- [Fig. 2(e)]. These conclusions are verified by analytical calculations (see SM [27]) showing that the factor a by which a catalyst reduces the activation energy satisfies

$$a \geq \frac{1}{2} + \max\left(0, \frac{h_s^+ - h_s^-}{2h_s^+}\right), \qquad (3)$$

which implies $a \geq 1/2$, with $a = 1/2$ reachable only if $h_s^- \geq h_s^+$. This analytical result is obtained in the limit $h_s^+ \gg 1$, but analyzing the lattice model shows that it also provides an upper bound on the catalytic efficiency η for large but finite values of h_s^+ (Fig. S1 of SM [27]).

To try to go beyond the limit of Eq. (3), several extensions of the model may be contemplated. For instance, we may consider the two binding sites to have different binding energies $\epsilon_{cs}^1 \neq \epsilon_{cs}^2$. However, the site with highest energy that most lowers h_s^+ is also inevitably the one that most limits release, implying a symmetric optimum with $\epsilon_{cs}^1 = \epsilon_{cs}^2$ (SM and Fig. S2 [27]). Alternatively, we may consider relaxing the assumption that the binding sites are fixed. For instance, we may assume them to fluctuate between a conformation with $L_c = 2$ and another with $L_c = 1$, possibly with an energy difference ϵ_c. This is the type of flexibility "along the reaction coordinate" considered in previous models [18,19], and we verify again here that it is detrimental to catalysis (SM and Fig. S3 [27]). This is simply explained: only when $L_c = 2$ is the energy barrier from $d_s = 1$ and $d_s = 2$ effectively lowered.

Catalysis with a discriminative switch.—The limitation expressed by Eq. (3) is in sharp contrast with the evidence that some enzymes can effectively totally annihilate activation barriers [22], which in our model corresponds to $a = 0$. This indicates that breaking the trade-offs of Sabatier principle is possible but by a mechanism that must differ from those considered previously.

We demonstrate here such a mechanism, which we call a discriminative switch. In this design, the catalyst can be in two states, C_0 and C_1, with the latter having a larger energy ϵ_c. These internal states are represented in our model by a third particle confined to two additional lattice sites while the two binding sites are kept at the same fixed locations [Fig. 3(a)]. The internal states are coupled to the reaction without compromising the geometry or rigidity of the binding sites themselves. This is achieved by interaction energies that depend on the internal state of

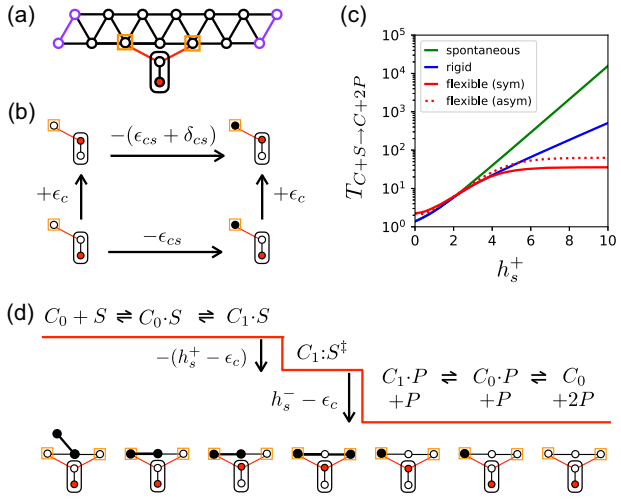

FIG. 3. Model for catalysis with a discriminative switch. (a) We add a degree of freedom in the form of a red particle that can take two positions, down (C_0) or up (C_1). (b) Switching from C_0 to C_1 involves an energy cost ϵ_c, and the interaction energy at each binding site is ϵ_{cs} in C_0 but $\epsilon_{cs}+\delta_{cs}$ in C_1. (c) Mean time of completion of the reaction in the absence of catalyst (green line), in the presence of an optimal rigid catalyst (blue line), a flexible symmetric catalyst with $\epsilon_{cs}=0$ and $\epsilon_c=\delta_{cs}=(h_s^++h_s^-)/2$ (full red line), or a flexible asymmetric catalyst with $\epsilon_{cs}^1=\epsilon_{cs}^2=0$, $\epsilon_c=\delta_{cs}^1=4h_s^+$ and $\delta_{cs}^2=1.5h_s^+$ (dotted red line). For large h_s^+, $T_{C+S\to C+2P}$ scales as $e^{ah_s^+}$, where $a=1$ without catalyst, $a\geq 1/2$ with rigid catalysts, but $a=0$ with catalysts having a discriminative switch (with h_s^- taken to be $h_s^-=2h_s^+$). Standard deviations can also be computed to show that the distributions of first-passage times are increasingly distinct as h_s^+ increases (Fig. S5 [27]). (d) When the conditions given in Eq. (4) are satisfied, the energy along the path from C_0+S to C_0+2P does not increase at any step. Catalysis is then barrierless. Examples of configurations along this path are illustrated at the bottom.

the catalyst: when in state C_0, the binding energy is as before ϵ_{cs}, but when in state C_1, an additional contribution brings it to $\epsilon_{cs}+\delta_{cs}$ [Fig. 3(b)]. In our model, δ_{cs} may be thought as arising from the interaction with the third particle which is brought closer to the binding sites in state C_1. In enzymes, this could correspond to additional interactions arising when a surface loop that is flexible in an open state C_0 comes to surround the substrate in a closed state C_1, with an associated entropy loss ϵ_c.

The key is then to make the following four choices that guarantee that no step involves a positive energy barrier: (1) $\epsilon_c=\delta_{cs}$ so that the transitions between states where a single site is bound, $C_0{\cdot}S \rightleftharpoons C_1{\cdot}S$ and $C_0{\cdot}P \rightleftharpoons C_1{\cdot}P$, are barrierless; (2) $\delta_{cs}\geq h_s^+$ so that accessing $S^\ddagger$ through $C_1{\cdot}S \to C_1{:}S^\ddagger$ involves a reduction of energy; (3) $\delta_{cs}\leq h_s^-$ so that no up-hill barrier is introduced for $C_1{:}S^\ddagger \to C_1{\cdot}P+P$; and (4) $\epsilon_{cs}=0$ so that release $C_0{\cdot}P+P \rightleftharpoons C_0+2P$ is barrierless. With such parameters, i.e., with

$$\epsilon_{cs}=0 \quad \text{and} \quad h_s^+\leq\delta_{cs}=\epsilon_c\leq h_s^-, \tag{4}$$

a path from C_0+S to C_0+2P is defined along which the energy of the system does not increase at any step [Fig. 3(d)], provided $h_s^+<h_s^-$.

These arguments are borne out by numerical and analytical calculations that follow the same principles as previously, with the internal state of the catalyst treated as a third particle. This is illustrated in Fig. 3(c), where $T_{C+S\to C+2P}$ in the presence of the catalyst of Fig. 3(a) is found to plateau as h_s^+ increases, consistent with $T_{C+S\to C+2P}\sim e^{ah_s^+}$ with $a=0$ (barrierless catalysis).

A variant of the model can also be defined where the two binding sites are not equivalent but have different parameters $\epsilon_{cs}^1,\delta_{cs}^1$ and $\epsilon_{cs}^2,\delta_{cs}^2$. This leads to different conditions for barrierless catalysis (see SM [27]):

$$\epsilon_{cs}^1=0, \qquad \epsilon_{cs}^2\leq 0, \qquad \delta_{cs}^2\leq\delta_{cs}^1=\epsilon_c,$$
$$\text{and} \quad h_s^+\leq\epsilon_{cs}^2+\delta_{cs}^2\leq h_s^- \tag{5}$$

(or the same conditions with the roles of sites 1 and 2 reversed). Here, $\epsilon_{cs}^1=0$ and $\delta_{cs}^1=\epsilon_c$ guarantee barrierless transitions $C_0+S \rightleftharpoons C_0{\cdot}S \rightleftharpoons C_1{\cdot}S$ and $C_1{\cdot}P+P \rightleftharpoons C_0{\cdot}P+P \rightleftharpoons C_0+2P$ (with binding at site 1) while $h_s^+\leq\epsilon_{cs}^2+\delta_{cs}^2$ guarantees that $C_1{\cdot}S\to C_1{:}S^\ddagger$ is downhill. The additional constraint $\delta_{cs}^2\leq\epsilon_c$ is necessary to prevent a particle to be stuck at binding site 2. It is indeed generally not sufficient to have a barrierless path from reactant to products for barrierless catalysis to occur as alternative paths may be present that lead to kinetic traps. This asymmetric design also achieves barrierless catalysis [Fig. 3(c)] although with a lower catalytic efficiency (Fig. S4 [27]), but it is more comparable to enzymes whose substrates are typically asymmetric and where a distinction is usually made between a "binding site" (site 1) and an "active site" (site 2).

Conclusion.—Based on the formulation and solution of an elementary model of catalysis, we have illustrated how a particular form of flexibility involving a two-state switch can overcome the limitations of rigid catalysis and effectively enable barrierless catalysis, where the activation energy of the spontaneous reaction is totally annihilated. The expression for the bound on rigid catalysis given by Eq. (3) is specific to our model but reflects a fundamental trade-off widely observed in heterogeneous catalysis where it is known as Sabatier principle [21]. The mechanism that we demonstrated, by which this bound can be overcome with a switch involving a compensation between two large (free) energies (ϵ_c and δ_{cs}), is generic and directly echoes the proposal that biological catalysts differ from nonbiological catalysts by their use of an "intrinsic binding energy" [5]. This concept has been illustrated in enzymes [14] and ribozymes [31], but its links to catalytic rate enhancements, product release, and conformational changes have never been fully explained, as reflected by the controversies over the role of flexibility in enzyme

catalysis [11–13] and the absence of this concept in reflections to overcome Sabatier principle in heterogeneous catalysis [32]. Our model clearly exposes these different links. Finally, from a physics standpoint, our modeling approach and our results are of interest for studying the many physical phenomena involving a coupling between a chemical reaction and a conformational change.

I am grateful to C. Nizak, M. Muñoz Basagoiti, Y. Sakref, Z. Zeravcic, and I. Junier for discussions and to ANR-21-CE45-0033 for funding.

[1] J. Greeley, Theoretical heterogeneous catalysis: Scaling relationships and computational catalyst design, Annu. Rev. Chem. Biomol. Eng. **7**, 605 (2016).
[2] J. K. M. Sanders, Supramolecular catalysis in transition, Chem. Eur. J. **4**, 1378 (1998).
[3] Dan S. Tawfik, Zelig Eshhar, and Bernard S. Green, Catalytic antibodies: A critical assessment, Mol. Biotechnol. **1**, 87 (1994).
[4] S. L. Lovelock, R. Crawshaw, S. Basler, C. Levy, D. Baker, D. Hilvert, and A. P. Green, The road to fully programmable protein catalysis, Nature (London) **606**, 49 (2022).
[5] W. P. Jencks, Advances in enzymology and related areas of molecular biology, Adv. Enzymol. Relat. Areas Mol. Biol. **43**, 219 (1975).
[6] A. J. Kirby, F. Hollfelder, and D. S. Tawfik, Nonspecific catalysis by protein surfaces, Applied biochemistry and biotechnology **83**, 173 (2000).
[7] G. Swiegers, *Mechanical Catalysis: Methods of Enzymatic, Homogeneous, and Heterogeneous Catalysis* (John Wiley & Sons, New York, 2008).
[8] J. R. Knowles, Enzyme catalysis: Not different, just better, Nature (London) **350**, 121 (1991).
[9] K. A. Henzler-Wildman, V. Thai, M. Lei, M. Ott, M. Wolf-Watz, T. Fenn, E. Pozharski, M. A. Wilson, G. A. Petsko, M Karplus, C. G. Hübner, and D Kern, Intrinsic motions along an enzymatic reaction trajectory, Nature (London) **450**, 838 (2007).
[10] L. Pauling, Molecular architecture and biological reactions, Chem. Eng. News **24**, 1375 (1946).
[11] S. C. L. Kamerlin and A. Warshel, At the dawn of the 21st century: Is dynamics the missing link for understanding enzyme catalysis?, Proteins **78**, 1339 (2010).
[12] A. Kohen, Role of dynamics in enzyme catalysis: Substantial versus semantic controversies, Acc. Chem. Res. **48**, 466 (2015).
[13] P. K. Agarwal, A biophysical perspective on enzyme catalysis, Biochemistry **58**, 438 (2019).
[14] J. P. Richard, Protein flexibility and stiffness enable efficient enzymatic catalysis, J. Am. Chem. Soc. **141**, 3320 (2019).
[15] G. R. Welch, B. Somogyi, and S. Damjanovich, The role of protein fluctuations in enzyme action: A review, Prog. Biophys. Molec. Biol. **39**, 109 (1982).
[16] V. S. Pande, A. Y. Grosberg, and T. Tanaka, Statistical mechanics of simple models of protein folding and design. Biophys. J. **73**, 3192 (1997).
[17] E. Rouviere, R. Ranganathan, and O. Rivoire, On the emergence of single versus multi-state allostery, arXiv: 2111.09377.
[18] O. Rivoire, Geometry and flexibility of optimal catalysts in a minimal elastic model, J. Phys. Chem. B **124**, 807 (2020).
[19] M. Muñoz-Basagoiti, O. Rivoire, and Z. Zeravcic, Computational design of a minimal catalyst using colloidal particles with programmable interactions, Soft Matter **19**, 3933 (2023).
[20] P. Sabatier, La catalyse en chimie organique, *Libraire Polytechnique* (1913).
[21] A. J. Medford, A. Vojvodic, and J. S. Hummelshøj, From the Sabatier principle to a predictive theory of transition-metal heterogeneous catalysis, J. Catal. **328**, 36 (2015).
[22] J. R. Knowles and W. J. Albery, Perfection in enzyme catalysis: The energetics of triosephosphate isomerase, Acc. Chem. Res. **10**, 105 (1977).
[23] Jacques Ninio, Alternative to the steady-state method: Derivation of reaction rates from first-passage times and pathway probabilities, Proc. Natl. Acad. Sci. U.S.A. **84**, 663 (1987).
[24] A. F. Voter, Introduction to the kinetic Monte Carlo method, in *Radiation Effects in Solids* (Springer, New York, 2007), pp. 1–23.
[25] S. Redner, *A Guide to First-Passage Processes* (Cambridge University Press, Cambridge, England, 2001).
[26] S. Iyer-Biswas and A Zilman, First-passage processes in cellular biology, Adv. Chem. Phys. **160**, 261 (2016).
[27] See Supplemental Material at http://link.aps.org/supplemental/10.1103/PhysRevLett.131.088401 for additional text and figures.
[28] Wei Zhang, Asymptotic analysis of multiscale Markov chain, arXiv:1512.08944.
[29] G. Pavliotis and A. Stuart, *Multiscale Methods: Averaging and Homogenization* (Springer Science & Business Media, New York, 2008).
[30] T. Bligaard, J. K. Nørskov, S. Dahl, J. Matthiesen, C. H. Christensen, and J. Sehested, The Brønsted-Evans-Polanyi relation and the volcano curve in heterogeneous catalysis, J. Catal. **224**, 206 (2004).
[31] K. J. Hertel, A. Peracchi, O. C. Uhlenbeck, and D. Herschlag, Use of intrinsic binding energy for catalysis by an RNA enzyme, Proc. Natl. Acad. Sci. U.S.A. **94**, 8497 (1997).
[32] J. Pérez-Ramírez and N. López, Strategies to break linear scaling relationships, Nat. Catal. **2**, 971 (2019).